SciMedCentral

Journal of Drug Design and Research

Research Article

QSAR Analysis of Tipifarnib Analogues for Anti-Chagas Disease

Rakhi Gawali[1]*, Sumer Thakur[2], Vijay H Masand[3], Rani Phadatare[4], and Arati Diwate[5]

[1]*Department of Chemistry, DBF Dayanand College of Arts & Science, India*
[2]*Department of Chemistry, RDIK and NKD College, Badnera-Amravati, Maharashtra, India*
[3]*Department of Chemistry, Vidya Bharati Mahavidyalaya, Amravati 444602, Maharashtra, India*
[4]*Department of Chemistry, Government Polytechnic College, India*
[5]*Sangameshwar College, India*

***Corresponding author**
Rakhi Gawali, Department of Chemistry, DBF Dayanand College of Arts & Science, Solapur-413002, Maharashtra, India, Tel no: +919822274626

Submitted: 03 November 2023
Accepted: 24 November 2023
Published: 25 November 2023
ISSN: 2379-089X

Keywords
- QSAR
- Tipifarnib
- Anti-Chagas Disease
- Drug Designing

Abstract

The cancer drug trial candidate Tipifarnib and its derivatives were subjected to a thorough QSAR analysis in the current study for the undertreated disease anti-Chagas. The study was effective in identifying the crucial structural elements that regulate the anti-Chagas profile of tipifarnib derivatives as a potential treatment. The genetic algorithm-multilinear regression (GA-MLR) method was used to create many models employing multiple splits in order to determine the greatest number and set of significant molecular descriptors. The created QSAR models have R2 > 0.85, Q2 > 0.82, and R2ext > 0.90, making them tri-parametric and statistically robust. The models are both internally and externally predictively strong. The models show a correlation between nitrogen's interaction with lipophilic atoms and the anti-Chagas activity of tipifarnib analogues.

ABBREVIATIONS

QSAR = Quantitative Structure-Activity Relationship; GA-MLR= Genetic Algorithm-Multilinear Regression; CYP51 = Cytochrome P450 51; ADMET = Absorption; Distribution; Metabolism; Excretion; and Toxicity; EC_{50} = Median Effective Concentration; pEC50 = negative logarithm of the EC_{50}; OECD = Organisation for Economic Co-operation and Development; GA = Genetic Algorithm; CV = Cross-validation; LOO = Leave-one-out; LMO = Leave-many-out; AD = Applicability Domain; FSM = Full Set Model; RMSE = Root Mean Square Error ; MAE = Maximal Absolute Error; MSA = Molecular Surface Area

INTRODUCTION

Chagas disease commonly spread by contact with an infected triatomine bug also known as "Kissing bug," "Benchuca," "Vinchuca," "Chinche," or "Barbeiro," is one of the most underdiagnosed parasitic diseases that can lead to life-threatening cardiac and stomach conditions [1]. It is often communicated through contact with an infected triatomine bug. Each year, the disease affects about ten million individuals, with the majority of cases concentrated in tropical areas like Africa and Latin America [2]. The protozoan parasite Trypanosoma cruzi (T. cruzi), a kinetoplastid hemoflagellate, is the cause of Chagas disease. Because there is no effective treatment available during the chronic stage of the illness, those who have been infected typically become a permanent host to the parasite. Nitrofuran, nifurtimox, benznidazole, and nitroimidazole are only a few of the very toxic medications that are commonly used in chemotherapy. The situation has worsened with the advent of resistance against nifurtimox [1,3-7]. Therefore, search for a new therapeutic agent or modification of existing one to curb Chagas disease is essential [8,9].

T. cruzi was recently discovered to be successfully inhibited by tipifarnib, a well-known anti-cancer drug created by Johnson & Johnson Pharmaceuticals [1]. The inhibition of endogenous sterol biosynthesis and binding to recombinant T. cruzi CYP51 provided further evidence that the target enzyme, CYP51, was implicated in the mechanism of bio-action in T. cruzi. T. cruzi amastigotes, which are the stage of the parasite's life cycle that develop in mammalian host cells, use ergosterol as a crucial component in the creation of their membranes because they are unable to utilise cholesterol from the host cells. It is a desirable lead molecule due to a number of benefits including excellent oral bioavailability, acceptable pharmacokinetic characteristics, and good human tolerance. But because tipifarnib has a chiral centre, it can exist in two stable isomeric forms [1]. Therefore, choosing a therapeutic candidate would require a separate examination of the pharmacokinetic and toxicity characteristics of both molecules. Additionally, it binds to the human protein farnesyl

transferase, which poses a hazardous problem for the use of tipifarnib as a T. cruzi inhibitor. To increase its potential as a drug candidate against T. cruzi, these problems must be resolved. Tipifarnib needs to be further optimized in order to remain a potent T. cruzi inhibitor with the appropriate ADMET profile. In order to continue the optimization, it would be appealing to create QSAR (Quantitative structure-activity relationship) models using the data that is now available for the detection of lead/drug similarity properties. For the purpose of identifying the pharmacophoric patterns and structural characteristics that control the bio-activity profile of congeneric series of compounds, QSAR is a well-known chemometric approach [10-14]. It is a ligand-based approach to drug design that heavily relies on mathematical, statistical, and algorithmic techniques combined with computer science. For example, risk assessment, toxicity prediction, and drug/lead optimisation have all been successful uses of QSAR [15-18].

In the current study, a thorough QSAR analysis was conducted to identify the structural characteristics that control tipifarnib and its analogues' anti-Chagas action.

Experimental methodology

Data set: The data set includes 33 Tipifarnib analogues with various substituents at various locations [1]. The electron-donating/-withdrawing groups in the substituents cause a positive alteration in the molecules' steric and electrostatic profiles (Table 1, Figure 1). The T. cruzi amastigote was used to test the Tipifarnib analogues. Prior to QSAR analysis, the EC50 (nM) values were transformed to pEC50 (M) values [16,17]. Table 1 lists the structures, EC50 (nM), and pEC50 (M).

QSAR methodology

The standard methodology and guidelines recommended and put into practise by many researchers and the OECD (Organisation for Economic Co-operation and Development) have been followed in the current work for successful QSAR analysis [10-12, 18-20]. The structures were created using the free ChemSketch 10 software, and then the energy consumption was reduced using TINKER and MMFF94 (Cut-off: 0.01). Then, a large number of descriptors were calculated using PowerMV, CDK and PADEL, PyDescriptor (a custom PyMOL plugin), and e-Dragon. More than 29,000 different 1D- to 3D -descriptors are included in the descriptor pool. After removing the constant, almost constant, highly correlated (|R| > 0.80), and redundant variables using objective feature selection in QSARINS 2.2.4 using default settings [21], Weka's genetic algorithm (GA) was used to conduct a heuristic search for selecting subjective features using default settings, except number of generations =10000 and number of features = 3. The data set was split into training (80%) and prediction (20%) sets at random for external validation before feature (descriptor) selection [18]. To obtain the most information possible, numerous splittings were used to generate multiple models.

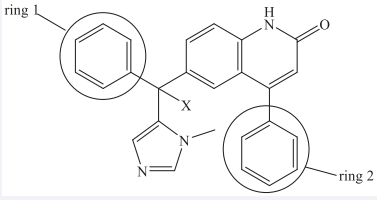

Figure 1 Tipifarnib analogues with a variety of substituents at different positions

Validation of the model: Effective QSAR model creation requires model validation. Therefore, for the purpose of model validation, OECD rules and suggested threshold values for a number of statistical parameters were used. The following characteristics were often taken into account: Using the prediction set, data randomization, or Y-scrambling, cross-validation (CV) via leave-one-out (LOO) and leave-many-out (LMO) procedures, and (d) determining whether the following requirements are met [16-19]: $R^2_{tr} \geq 0.6$, $Q^2_{loo} \geq 0.5$, $Q^2_{LMO} \geq 0.6$, $R^2 > Q^2$, $R^2_{ex} \geq 0.6$, $RMSE_{tr} < RMSE_{cv}$, $\Delta K \geq 0.05$, $CCC \geq 0.80$, $Q^2\text{-}F^n \geq 0.60$, $r^2_m \geq 0.6$, $(1\text{-}r^2/r_o^2) < 0.1$, $0.9 \leq k \leq 1.1$ or $(1\text{-}r^2/r'^2_o) < 0.1$, $0.9 \leq k' \leq 1.1$,$| r_o^2 - r'^2_o | < 0.3$ with *RMSE* and *MAE* close to zero. Any model not satisfying these criteria were subsequently rejected.

Applicability Domain (AD): AD assessment of a QSAR model is essential criterion for QSAR model development. In the present work, Williams plot have been plotted to assess the AD of the developed model. QSARINS-Chem 2.2.1 was used for getting the Williams plot using the default setting [11-14].

RESULTS AND DISCUSSION

Our team recently demonstrated that using multiple modelling to capture less-privileged chemical characteristics is a wise decision. Therefore, to ensure the capture of dominant and less prominent structural features that influence the bio-activity of PBIs, the same stated technique has been applied in the current study. As a result, various QSAR models were created utilising both the entire data set (referred to in the present study as the full set model, or FSM) and the divided data set (80% training and 20% prediction sets). The data set was randomly divided before model building when employing a divided data set to prevent developer bias in choosing the training and prediction sets. One model's prediction set for a chemical might or might not include it. QSARINS-Chem 2.2.1 was operating with the default parameters for OFS and SFS. The heuristic search for variables was restricted for simplicity to a collection of only three descriptors. There was no appreciable improvement in the statistical quality of the model after three variables. The following are the statistical parameters for the tri-parametric GA-MLR models:

Model-1 (FSM)

pEC_{50} = 20.013 (± 3.350) + 3.285 (± 1.131) * O_don_8Ac – 0.563 (± 0.249) * N_lipo_5B – 0.009 (± 0.003) * QXXm

N_{tr} = 33, Q^2_{loo} = 0.823, R^2_{tr} = 0.865, R^2_{adj} = 0.851, K_{xx} = 0.310, ΔK = 0.203, $RMSE_{tr}$ = 0.315, $RMSE_{cv}$ = 0.358, s = 0.336, F = 61.714, CCC_{tr} = 0.927, CCC_{cv} = 0.906, MAE_{tr} = 0.264, MAE_{cv} = 0.301, Q^2_{LMO} = 0.820

Table 1: Experimental EC_{50}, and substituents on Tipifarnib analogues used in the present study

S.N.	*T. cruzi* EC_{50} (nM)	X	ring 2	ring 1	Imidazole
1	4	NH_2	3-chloro	4-chloro	1-methyl-1H-imidazole
2	0.6	OMe	3-chloro-2-methyl	4-chloro	1-methyl-1H-imidazole
3	3.1	OMe	3-chloro	4-chloro	1-methyl-1H-imidazole
4	0.7	OMe	2-methyl	4-chloro	1-methyl-1H-imidazole
5	0.8	OMe	2-trifluoromethyl	4-chloro	1-methyl-1H-imidazole
6	1.1	OMe	3-fluoro	4-chloro	1-methyl-1H-imidazole
7	1.2	OMe	3-methyl	4-chloro	1-methyl-1H-imidazole
8	12	OMe	3-trifluoromethyl	4-chloro	1-methyl-1H-imidazole
9	0.8	OMe	2-fluoro	4-chloro	1-methyl-1H-imidazole
10	0.8	OMe	phenyl	4-chloro	1-methyl-1H-imidazole
11	0.82	OMe	4-chloro	4-chloro	1-methyl-1H-imidazole
12	0.5	OMe	4-fluoro	4-chloro	1-methyl-1H-imidazole
13	2	OMe	4-methyl	4-chloro	1-methyl-1H-imidazole
14	1.8	OMe	2,6-dimethyl	4-chloro	1-methyl-1H-imidazole
15	3.21	OMe	2,6-dichloro	4-chloro	1-methyl-1H-imidazole
16	0.31	OMe	2,6-difluoro	4-chloro	1-methyl-1H-imidazole
17	1.4	OMe	3,5-dimethyl	4-chloro	1-methyl-1H-imidazole
18	2.2	OMe	3-chloro	naphthyl	1-methyl-1H-imidazole
19	17	OH	3-chloro	4-chloro	1-methyl-1H-imidazole
20	112	OH	3-chloro-2-methyl	4-chloro	1-methyl-1H-imidazole
21	27	OEt	3-chloro-2-methyl	4-chloro	1-methyl-1H-imidazole
22	69	OPr	3-chloro-2-methyl	4-chloro	1-methyl-1H-imidazole
23	5	NHMe	3-chloro-2-methyl	4-chloro	1-methyl-1H-imidazole
24	118	NH_2	3-chloro	4-chloro	1-ethyl-1H-imidazole
25	100	NHMe	3-chloro	4-chloro	1-ethyl-1H-imidazole
26	3	OMe	3-chloro	4-chloro	1-ethyl-1H-imidazole
27	228	OH	3-chloro	4-chloro	1-ethyl-1H-imidazole
28	3	OMe	3-chloro	4-methyl	1-methyl-1H-imidazole
29	5	OMe	3-chloro	4-trifluoromethyl	1-methyl-1H-imidazole
30	10	OMe	3-chloro	4-ethyl	1-methyl-1H-imidazole
31	33	OMe	3-chloro	4-cumene	1-methyl-1H-imidazole
32	320	OMe	3-phenyl	4-chloro	1-methyl-1H-imidazole
33	83	OMe	3-benzene	4-chloro	1-methyl-1H-imidazole

Model-2 (Divided data set)

pEC_{50} = 20.993 (± 3.988) – 0.095 (± 0.044) * da_H_9B – 0.540 (± 0.289) * N_lipo_5B – 0.010 (± 0.003) * QXXm

N_{tr} = 27, N_{ex} = 6, Q^2_{loo} = 0.831, R^2_{tr} = 0.870, R^2_{adj} = 0.853, K_{xx} = 0.303, ΔK = 0.202, $RMSE_{tr}$ = 0.306, $RMSE_{cv}$ = 0.348, $RMSE_{ex}$ = 0.394, s = 0.331, F = 51.151, Q^2-F^1 = 0.809, Q^2-F^2 = 0. 0.801, Q^2-F^3 = 0.783, CCC_{tr} = 0.930, CCC_{cv} = 0.909, CCC_{ex} = 0.897, r^2m av = 0.794, r^2m de = 0.093, MAE_{tr} = 0.249, MAE_{cv} = 0.288, MAE_{ex} = 0.338, R^2_{ext} = 0.918, Q^2_{LMO} = 0.811

Model-3 (Divided data set)

pEC_{50} = 35.716 (± 9.621) – 0.319 (± 0.182) * accminus_MSA – 0.690 (± 0.261) * N_lipo_5B – 0.010 (± 0.003) * QXXm

N_{tr} = 27, N_{ex} = 6, Q^2_{loo} = 0.837, R^2_{tr} = 0.870, R^2_{adj} = 0.853, K_{xx} = 0.470, ΔK = 0.077, $RMSE_{tr}$ = 0.291, $RMSE_{cv}$ = 0.325, $RMSE_{ex}$ = 0.451, s = 0.315, F = 51.403, Q^2-F^1 = 0.826, Q^2-F^2 = 0. 0.756, Q^2-F^3 = 0.688, CCC_{tr} = 0.931, CCC_{cv} = 0.913, CCC_{ex} = 0.885, r^2m av = 0.698, r^2m de = 0.069, MAE_{tr} = 0.243, MAE_{cv} = 0.280, MAE_{ex} = 0.373, R^2_{ext} = 0.786, Q^2_{LMO} = 0.794

The statistical symbols have their typical meanings, which are also provided in the accompanying data. Table 2 displays the pEC50 values as well as the descriptor values that were employed. Based on the statistical characteristics, it appears that the produced models have good internal fitting and meet the cutoff values for a number of statistical parameters that are crucial for determining internal resilience and external predictability. The models' strong external prediction capacity is indicated by the high value of several external validation parameters, including CCCex, Q2-Fn, R2ext, etc., and the low values of RMSE, s, and MAE, etc. An adequate number of descriptors are present in the model, according to the close value of R2adj. And R2. Similar to how similar R2 and Q2 values indicate that the models do not exhibit over-fitting. The low value of *RMSE* and *MAE* (fitting, cross-validation and external validation) specifies that the developed models have statistical acceptability.

DISCUSSION

In the developed models, the common descriptor is QXXm, which is a geometrical descriptor and corresponds to COMMA2 value/weighted by atomic masses activity, has negative correlation with the activity. Therefore, its value must be kept

Table 2: Values of molecular descriptors and pEC_{50} for the data set

S. N.	pEC_{50}	QXXm	da_H_9B	N_lipo_5B	O_don_8Ac	accminus_MSA
1.	8.398	311.237	13	16	0	43.06295
2.	9.222	326.92	13	15	0	41.51342
3.	8.509	320.129	11	15	0	41.54747
4.	9.155	257.504	14	15	0	41.98221
5.	9.097	297.908	11	15	0	41.87246
6.	8.959	278.501	11	15	0	42.02498
7.	8.921	271.578	14	15	0	41.87778
8.	7.921	360.145	11	15	0	41.92143
9.	9.097	257.09	11	15	0	41.81082
10.	9.097	248.193	12	15	0	41.99664
11.	9.086	286.032	11	15	0	41.99585
12.	9.301	286.032	11	15	0	41.99585
13.	8.699	280.88	14	15	0	41.81427
14.	8.745	267.324	16	15	0	42.11884
15.	8.493	299.339	10	15	0	42.05618
16.	9.509	268.724	10	15	0	42.17695
17.	8.854	292.784	16	15	0	42.09243
18.	8.658	313.751	11	15	0	41.84568
19.	7.77	314.262	21	15	-0.3736	44.85659
20.	6.951	321.68	23	15	-0.3736	44.99809
21.	7.569	344.106	13	16	0	41.52892
22.	7.161	373.782	13	16	0	41.96532
23.	8.301	312.637	14	16	0	40.64602
24.	6.928	349.198	13	17	0	42.45161
25.	7	362.533	12	17	0	40.60624
26.	8.523	347.097	11	16	0	41.05926
27.	6.642	356.071	23	16	-0.3736	44.61465
28.	8.523	319.429	11	16	0	41.21349
29.	8.301	342.56	11	16	0	41.09026
30.	8	319.508	11	16	0	41.30114
31.	7.481	328.818	11	16	0	41.29695
32.	6.495	481.969	13	16	0	40.76464
33.	7.081	439.806	13	16	0	41.2677

as low as possible to enhance the activity. The second common descriptor N_lipo_5B (number of lipophilic atoms within five bonds from Nitrogen atoms) has negative coefficient in all the developed models. Hence, the value of this descriptors must be restricted for enhanced activity. da_H_9B corresponds to number of Hydrogen atoms within nine bonds from such a group which can act as H-bond donor as well as acceptor such as -OH, $-NH_2$, etc. the negative coefficient for this descriptor in model 2 indicates that lowering the value of this descriptor would result in better activity profile.

A molecular descriptor with negative coefficient in model 3 is accminus_MSA (molecular surface area of negatively charged H-bond acceptor atoms). Therefore, the molecular surface area of negatively charged H-bond acceptor atoms must be constrained to increase the anti-Chagas activity. The molecular descriptors accminus_MSA, N_lipo_5B and da_H_9B have been depicted in Figure 2 using the most and least active molecules (molecule number 16 and 32), as the representatives only.

The only molecular descriptor with a positive coefficient in model 1 is O_don_8Ac, which stands for sum of partial charges on H-bond donor atoms which are present within 8Å from oxygen atoms. In case of compound number **2**, **3** and **26** the oxygen atom of -OMe group (with lesser negative charge) is within a distance of 8Å from oxygen atom of quinolinone moiety. Whereas for compound number **20**, **19** and **27**, though, the oxygen atom of -OH group is within a distance of 8Å from oxygen atom of quinolinone moiety but possesses a higher negative charge. This could be one of the possible reasons for better activity of **2** (EC_{50} = 0.6 nM) than **20** (EC_{50} = 112 nM), **3** (EC_{50} = 3.1 nM) than **19** (EC_{50} = 17 nM), and **26** (EC_{50} = 3 nM) than **27** (EC_{50} = 228 nM). This points out another observation that -OMe is a better substituent at -X than -OH for increasing the activity.

In Table 3, the status of the molecule, predicted and the residual values by developed models 1-3 have been tabulated.

The fitting curve, residual plot, Y-scrambling and Williams plots are available in the supporting information.

CONCLUSIONS

In conclusion, the robust QSAR models with good predictive ability indicate that activity has good relation with $-OCH_3$ group, lipophilic atoms within five bonds from Nitrogen atoms, presence

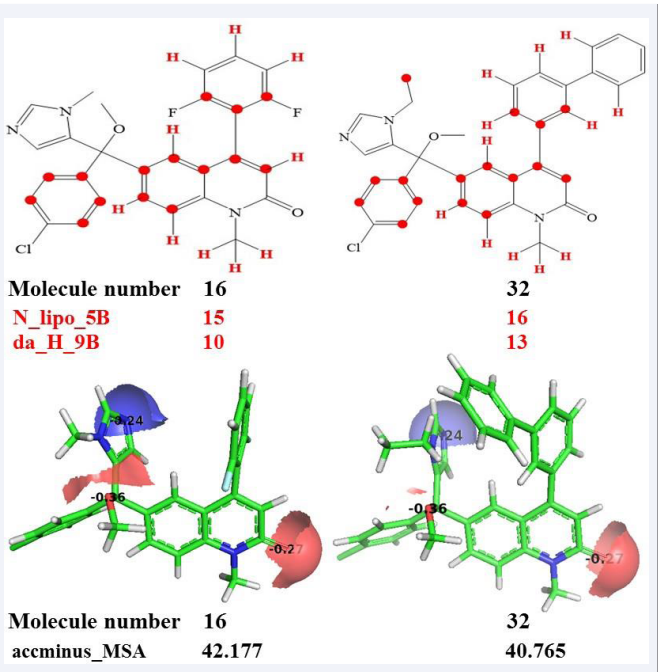

Figure 2 Representation of accminus_MSA, N_lipo_5B and da_H_9B using molecule number 16 (most active) and 32 (least active) as the representatives only (red filled circles for N_lipo_5B and red coloured hydrogen atoms for da_H_9B).

Table 3: Status of the molecule, predicted and the residual values by developed models 1-3

S.N.	Status Model-1	Pred. by model-1	Residual Model-1	Status Model-2	Pred. by model-2	Residual Model-2	Status Model-3	Pred. by model-3	Residual Model-3
1	Training	8.1521	-0.2459	Training	8.1220	-0.2760	Prediction	7.6498	-0.7482
2	Training	8.5704	-0.6516	Training	8.5100	-0.7120	Training	8.6691	-0.5529
3	Training	8.6328	0.1238	Training	8.7652	0.2562	Training	8.7298	0.2208
4	Training	9.2085	0.0535	Training	9.0858	-0.0692	Training	9.2510	0.0960
5	Training	8.8371	-0.2599	Prediction	8.9799	-0.1171	Training	8.8602	-0.2368
6	Training	9.0155	0.0565	Training	9.1673	0.2083	Training	9.0161	0.0571
7	Training	9.0791	0.1581	Training	8.9498	0.0288	Prediction	9.1360	0.2150
8	Training	8.2649	0.3439	Training	8.3786	0.4576	Training	8.1887	0.2677
9	Training	9.2123	0.1153	Training	9.3742	0.2772	Training	9.3101	0.2131
10	Training	9.2941	0.1971	Prediction	9.3653	0.2683	Training	9.3445	0.2475
11	Training	8.9463	-0.1397	Training	9.0946	0.0086	Training	8.9460	-0.1400
12	Training	8.9463	-0.3547	Training	9.0946	-0.2064	Training	8.9460	-0.3550
13	Training	8.9936	0.2946	Training	8.8599	0.1609	Prediction	9.0583	0.3593
14	Training	9.1183	0.3733	Training	8.8013	0.0563	Training	9.1039	0.3589
15	Training	8.8239	0.3309	Prediction	9.0608	0.5678	Training	8.7865	0.2935
16	Training	9.1054	-0.4036	Training	9.3566	-0.1524	Training	9.0706	-0.4384
17	Training	8.8842	0.0302	Training	8.5553	-0.2987	Training	8.8440	-0.0100
18	Training	8.6914	0.0334	Training	8.8268	0.1688	Training	8.7018	0.0438
19	Training	7.4593	-0.3107	Training	7.8738	0.1038	Training	7.7353	-0.0347
20	Training	7.3911	0.4401	Prediction	7.6125	0.6615	Prediction	7.6119	0.6609
21	Training	7.8499	0.2809	Training	7.8044	0.2354	Training	7.7931	0.2241
22	Training	7.5771	0.4161	Training	7.5177	0.3567	Training	7.3410	0.1800
23	Training	8.1392	-0.1618	Training	8.0137	-0.2873	Training	8.4066	0.1056
24	Training	7.2407	0.3127	Training	7.2158	0.2878	Training	6.7549	-0.1731
25	Training	7.1181	0.1181	Prediction	7.1817	0.1817	Training	7.2035	0.2035
26	Training	7.8224	-0.7006	Training	7.9652	-0.5578	Training	7.9115	-0.6115
27	Training	6.5125	-0.1295	Training	6.7408	0.0988	Prediction	6.6819	0.0399
28	Training	8.0768	-0.4462	Training	8.2325	-0.2905	Training	8.1539	-0.3691
29	Training	7.8641	-0.4369	Training	8.0090	-0.2920	Training	7.9494	-0.3516
30	Training	8.0761	0.0761	Prediction	8.2317	0.2317	Training	8.1250	0.1250
31	Training	7.9905	0.5095	Training	8.1418	0.6608	Training	8.0283	0.5473
32	Training	6.5825	0.0875	Training	6.4726	-0.0224	Training	6.5842	0.0892
33	Training	6.9701	-0.1109	Training	6.8799	-0.2011	Prediction	6.8680	-0.2130

of less negatively charged donor atom from oxygen atom of quinolinone ring and molecular surface area of negatively charged H-bond acceptor atoms.

AUTHOR CONTRIBUTIONS

R.G. and S.T.: conceptualization, project design, and experimental studies; R.G., S.T. and V.H.M.: drafting, resources, and funding management; R.G., S.T. and R.P.: data collection and curation, drafting, and data compilation; R.G., V.H.M. and R.P.: draft revision and analysis. All authors have read and agreed to the published version of the manuscript.

ACKNOWLEDGMENTS

Authors are grateful to Dr. Paola Gramatica and QSARINS developing team for providing QSARINS.

REFERENCES

1. Kraus JM, Tatipaka HB, McGuffin SA, Chennamaneni N, Karimi M, Arif J, et al. Second Generation Analogues of the Cancer Drug Clinical Candidate Tipifarnib for Anti-Chagas Disease Drug Discovery. J Med Chem. 2010; 53: 3887-5898.

2. Technical report of the TDR disesase reference group on Chagas Disease, Human African Trypanosomiasis and Leishmaniasis; World Health Organisation.

3. McKerrow JH, Doyle PS, Engel JC, Podust LM, Robertson SA, Ferreira R, et al. Two approaches to discovering and developing new drugs for Chagas disease. Mem Inst Oswaldo Cruz. 2009; 104: 263-269.

4. Patterson S, Wyllie S. Nitro drugs for the treatment of trypanosomatid diseases: past, present, and future prospects. Trends Parasitol. 2014; 30: 289-298.

5. Bern C, Kjos S, Yabsley MJ. Montgomery SP. Trypanosoma cruzi and Chagas 'disease in the United States. Clin Microbiol Rev. 2011; 24: 655-681.

6. Reyes PP, Vallejo M, Garcia MM, Garay AGG. Trypanocidal drugs for late stage, symptomatic Chagas disease (Trypanosoma cruzi infection). Cochrane Database Syst Rev. 2020; 12; CD004102.

7. Maya JD, Bollo S, Nunez-Vergara LJ, Squella JA, Repetto Y, Morello A, et al. Trypanosoma cruzi: Effect and mode of action of nitroimidazole and nitrofuran derivatives. Biochem Pharmacol. 2003; 65: 999-1006.

8. De Rycker M, Wyllie S, Horn D, Read KD, Gilbert IH. Anti-trypanosomatid drug discovery: progress and challenges. Nat Rev Microbiol. 2023; 21: 35-50.

9. Gabaldón-Figueira JC, Martinez-Peinado N, Escabia E, Ros-Lucas A, Chatelain E, Scandale I, et al. State-of-the-Art in the Drug Discovery Pathway for Chagas Disease: A Framework for Drug Development and Target Validation. Res Rep Trop Med. 2023; 14: 1-19.

10. Gramatica P. On the development and validation of QSAR models. Methods Mol Biol. 2013; 930: 499-526.

11. Kim JH, Gramatica P, Kim, MG, Kim D, Tratnyek PG. QSAR modelling of water quality indices of alkylphenol pollutants. SAR QSAR Environ Res. 2007; 18: 729-743.

12. Kovarich S, Papa E, Li J, Gramatica P. QSAR classification models for the screening of the endocrine-disrupting activity of perfluorinated compounds. SAR QSAR Environ Res. 2012; 23: 207-220.

13. Liu H, Gramatica P. QSAR study of selective ligands for the thyroid hormone receptor beta. Bioorg Med Chem. 2007; 15: 5251-5261.

14. Liu H, Papa E, Gramatica P. Evaluation and QSAR modeling on multiple endpoints of estrogen activity based on different bioassays. Chemosphere. 2008; 70: 1889-1897.

15. Mahajan DT, Masand VH, Patil KN, Ben Hadda T, Jawarkar RD, Thakur SD, et al. CoMSIA and POM analyses of anti-malarial activity of synthetic prodiginines. Bioorg Med Chem Lett. 2012; 22: 4827-4835.

16. Mahajan DT, Masand, VH, Patil KN, Hadda TB, Rastija V. Integrating GUSAR and QSAR analyses for antimalarial activity of synthetic prodiginines against multi drug resistant strain. Med Chem Res. 2012, 22, 2284-2292.

17. Martin TM, Harten P, Young DM, Muratov EN, Golbraikh A, Zhu H, et al. Does Rational Selection of Training and Test Sets Improve the Outcome of QSAR Modeling? J Chem Inf Model. 2012; 52: 2570-2578.

18. Masand VH, Jawarkar RD, Patil KN, Nazerruddin GM, Bajaj SO. Correlation potential of Wiener index and molecular refractivity vis-a`-vis Antimalarial activity of xanthone derivatives. Org Chem: An Ind J 2010; 6: 30-38.

19. Masand VH, Jawarkar RD, Mahajan DT, Hadda TB, Sheikh J, Patil KN. QSAR and CoMFA studies of biphenyl analogs of the anti-tuberculosis drug (6S)-2-nitro-6-{[4-(trifluoromethoxy) benzyl]oxy}-6,7-dihydro-5H-imidazo[2,1-b][1,3]oxazine(PA-824). Med Chem Res. 2012; 21: 2624-2629.

20. Masand VH, Mahajan DT, Patil KN, Hadda TB, Youssoufi MH, Jawarkar RD, et al. Optimization of Antimalarial Activity of Synthetic Prodiginines: QSAR, GUSAR, and CoMFA analyses. Chem Biol Drug. Des. 2013; 81: 527-536.

21. Zaki MEA, Al-Hussain SA, Bukhari SNA, Masand VH, Rathore MM, Thakur SD, et al. Exploring the Prominent and Concealed Inhibitory Features for Cytoplasmic Isoforms of Hsp90 Using QSAR Analysis. Pharmaceuticals. 2022; 15: 303.